Hunt for a Lifshitz point in single-crystalline UPd_2Si_2. I. High magnetic fields

Maria Szlawska,* Magdalena Majewicz, Konrad Wochowski, and Dariusz Kaczorowski
Institute of Low Temperature and Structure Research, Polish Academy of Sciences, ul. Okólna 2, 50-422 Wrocław, Poland

(Received 30 January 2024; accepted 8 July 2024; published 23 July 2024)

A single crystal of UPd_2Si_2 was studied in wide ranges of temperature and magnetic field strength with the main goal of revealing the existence of a Lifshitz point in its magnetic phase diagram. The experiments showed that the boundaries between paramagnetic, modulated antiferromagnetic, and uniform antiferromagnetic phases do not meet up to 14 T.

DOI: 10.1103/PhysRevB.110.014434

I. INTRODUCTION

The concept of a Lifshitz point (LP) was originally introduced in 1975 by Hornreich, Luban, and Shtrikman [1]. This special bicritical point can occur in various systems, such as magnetic compounds, liquid crystals, charge transfer salts, or structurally incommensurate materials [2]. In the case of magnetics, LP is a point at which a paramagnetic phase coexists with both a uniform (commensurate) phase and a modulated (incommensurate) phase. In other words, LP divides a continuous transition line between disordered and ordered phases into two segments. One part of the transition is from the paramagnetic to the uniform phase, while the other one is from the paramagnetic to the incommensurate phase. Despite the fact that modulated systems are common in nature, and in dissonance with quite extensive theoretical development [1], to date, the occurrence of LP in any magnetic material has been proven conclusively only for MnP [3].

The compounds with composition UT_2Si_2, where T is a d-electron transition element, crystallize mostly with the tetragonal $ThCr_2Si_2$-type unit cell (space group $I4/mmm$). The exceptions are UIr_2Si_2 and UPt_2Si_2 that adopt a primitive $CaBe_2Ge_2$-type structure (space group $P4/nmm$) [4]. The UT_2Si_2 silicides show large variety of physical behaviors, ranging from Pauli paramagnetism (for T = Fe, Re, Os) [5,6]. through a mysterious hidden-order state in URu_2Si_2 [7], to long-range magnetic ordering (for T = Cr, Mn, Co, Ni, Cu, Rh, Pd, Ir, Pt, Au) [8–20]. In all these materials (but UMn_2Si_2 [10]), the magnetic moment originates from the $5f$ electronic shell of U atoms. The observed differences in the magnetic ground states can be ascribed to different degrees of localization of $5f$ electrons [21]. Regardless of the magnetic structure, in each compound the magnetic moments are oriented along the c axis, which correlates well with the shortest U-U distance confined within the tetragonal plane.

The present paper was motivated by previous reports on UPd_2Si_2. The compound was reported to show a complex magnetic phase diagram, obtained with a magnetic field applied along the c axis that consists of four domains: paramagnetic (PM) and three different ordered phases [22,23]. In the phase diagram determined by Honma *et al.* [24], UPd_2Si_2 undergoes two magnetic phase transitions in zero external magnetic field. First, an incommensurate longitudinal sine wave magnetic structure (IC) forms below the Néel temperature $T_N = 135$ K, characterized by the modulation vector $Q = (0\ 0\ q_z)$ with q_z changing from 0.71 to 0.74. Then, at $T_1 = 108$ K, UPd_2Si_2 exhibits a first-order phase transition to a simple antiferromagnetic structure (AFM) with $Q = (0\ 0\ 1)$ [22,25]. The application of a magnetic field induces a ferrimagnetic ordering (FIM) with $Q = (0\ 0\ 2/3)$ [23]. A triple point, at which three ordered phases coexist, was observed at $\mu_0 H = 1.9$ T and $T = 107$ K [24]. Remarkably, in the more recent report by Plackowski *et al.* [26], a slightly different phase diagram of UPd_2Si_2 was presented, in which the FIM phase appeared already in zero magnetic field. There, a cascade of three magnetic transitions from PM to IC to FIM and eventually to AFM states was observed in zero field at $T_N = 136$ K, $T_{t1} = 96.5$ K, and $T_{t2} = 85$ K, respectively. The application of a magnetic field led to stabilization of the FIM phase and narrowing of the domain of the IC phase. Accordingly, it may be expected that in strong enough magnetic fields, the IC phase disappears at a point in which the boundaries between the PM, IC, and FIM phases meet. The authors of Ref. [26] hypothesized that this multicritical point can be LP. Interestingly, another way to create LP in UPd_2Si_2 is by possibly applying external pressure. According to the literature reports [27,28], the IC phase disappears under high pressure, and the boundary lines of the transitions PM to IC and IC to AFM meet at a pressure-induced LP.

With the main aim to verify the hypothesis of the existence of LP in the magnetic phase diagram of UPd_2Si_2, we have undertaken a thorough reinvestigation of the thermodynamic and electrical transport properties of the compound in strong magnetic fields and under high pressure. In this paper, we present the first part of our work, devoted to high magnetic field studies. Our results obtained under high pressure will be described in a companion paper [29].

II. EXPERIMENTAL DETAILS

A single crystal of UPd_2Si_2 was grown using the Czochralski pulling technique in a tetra-arc furnace (GES Corporation) under argon atmosphere. The starting constituents were

*Contact author: m.szlawska@intibs.pl

 ©2024 American Physical Society

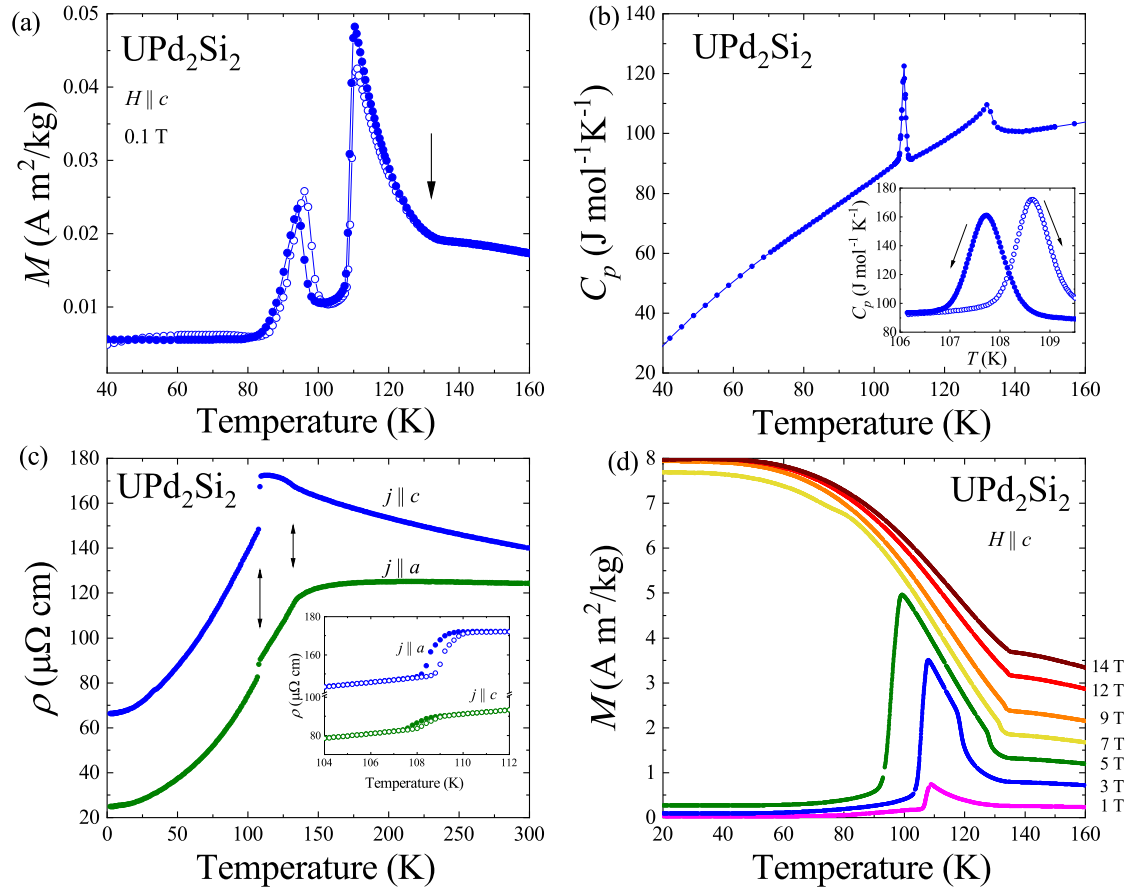

FIG. 1. (a) Temperature dependence of the magnetization in single-crystalline UPd_2Si_2 measured in a magnetic field of 0.1 T applied along the c axis. Open and solid symbols denote the data taken with increasing and decreasing temperature, respectively. The arrow marks T_N. (b) Temperature variation of the specific heat of single-crystalline UPd_2Si_2 measured in zero magnetic field. The inset presents the specific heat measured in the vicinity of T_1 on heating (open symbols) and cooling (solid symbols) the specimen. (c) Temperature dependencies of the electrical resistivity of single-crystalline UPd_2Si_2 measured with electric current flowing along the a axis and c axis. The arrows mark the transition temperatures described in the text. The inset presents the resistivity data collected in the vicinity of T_1 with increasing (open symbols) and decreasing (solid symbols) temperature. (d) Temperature variations of the magnetization in single-crystalline UPd_2Si_2 measured in various magnetic fields applied along the c axis upon cooling the sample in zero field.

high-purity elements (U-99.9%, Pd-99.99%, and Si-99.9999%). The obtained crystal was a rod of approximately 3 mm in diameter and 10 mm in length. No further heat treatment was applied. Chemical composition and homogeneity of the crystal was checked by energy dispersive x-ray analysis on an FEI scanning electron microscope equipped with an EDAX Genesis XM4 spectrometer. Crystallinity and orientation of the specimens cut for physical properties measurements were checked by the Laue backscattering technique using a Proto Laue-COS single-crystal orientation system.

Magnetic properties measurements were performed in the temperature range between 10 and 160 K in magnetic fields up to 7 T using a Quantum Design MPMS-7 superconducting quantum interference (SQUID) device, and up to 14 T employing a Quantum Design PPMS-14 platform equipped with a vibrating sample magnetometer (VSM) inset. The heat capacity was measured in the temperature interval 40–160 K and in magnetic fields up to 14 T, using the relaxation technique implemented in the PPMS-14 platform. In order to examine properly the sharp first-order phase transitions, in the vicinity of T_1 and T_2, the heat capacity was characterized by analyzing the slopes of long heat pulse.

The temperature and magnetic field variations of the electrical resistivity were studied from 2 to 300 K, in magnetic fields up to 14 T, employing a standard ac four-probe method. For these measurements, the same PPMS-14 platform was employed. In zero field, the resistivity was measured with electric current flowing either within the tetragonal plane and along the crystallographic c axis. The measurements in the magnetic field applied along the c axis were performed with the current flowing in the tetragonal plane.

III. EXPERIMENTAL RESULTS

The temperature dependence of the magnetization, $M(T)$, of UPd_2Si_2, measured in a magnetic field of 0.1 T applied along the c axis, is presented in Fig. 1(a). Below the Néel temperature $T_N = 132$ K, the magnetization starts to increase rapidly reaching a maximum at the transition from the IC to AFM state. The transition temperature $T_1 = 108$ K was defined as an inflection point in $M(T)$ (maximum in the

temperature derivative of the magnetization dM/dT). The variations measured with decreasing and increasing temperature show a narrow thermal hysteresis, confirming the first-order type of transition. Similarly to previous investigations [23,24], another sharp maximum can be seen in $M(T)$ near 95 K, which was attributed in those studies to a small amount of an unidentified impurity. In line with such a supposition, neither the specific heat nor electrical resistivity data collected for UPd_2Si_2 show any corresponding feature near this temperature (see below). Overall, it can be stated that the magnetic properties of the single crystal grown in the present work are very similar to those reported by Honma *et al.* [24].

The specific heat of UPd_2Si_2, $C_p(T)$, measured as a function of the temperature in zero magnetic field, is presented in Fig. 1(b). There are two distinct features in $C_p(T)$, namely a λ-like anomaly at T_N and a sharp narrow maximum at T_1. The inset to the figure shows $C_p(T)$ measured close to T_1 by analyzing a long heat pulse. A thermal hysteresis of about 1 K in the position of the phase transition corroborates its first-order character.

The electrical resistivity probed as a function of the temperature, $\rho(T)$, in zero magnetic field along two main crystallographic directions is displayed in Fig. 1(c). In the paramagnetic state, the resistivity measured along the fourfold axis initially increases slightly with decreasing temperature, and $\rho(T)$ bends upwards below the Néel temperature. In turn, the in-plane resistivity in the paramagnetic region hardly changes and bends downwards near T_N. For both current directions, the order-order transition at T_1 manifests itself as a rapid drop in $\rho(T)$. As displayed in the insets to Fig. 1(c), the $\rho(T)$ variations exhibit clear thermal hysteresis at T_1, in concert with the magnetization and specific heat data.

Figure 1(d) illustrates the evolution of $M(T)$ with changing the magnetic field strength. As can be inferred from this figure, there is almost no change in the position of the bend associated with the onset of the ordered state. In turn, the maximum signaling the transition from the IC to AFM states at T_1 initially slightly shifts towards lower temperatures. In $\mu_0 H = 3$ T, due to the formation of the FIM phase, the shape of the $M(T)$ curve slightly changes, and two anomalies can be recognized at T_2 and T_3 that manifest the transitions from IC to FIM and from FIM to AFM states, respectively. With a further increase of the field strength, T_3 decreases, while T_2 increases. Above 7 T, the magnetization smoothly increases in the ordered state down to lowest temperatures, and the order-order phase transition at T_3 is no longer observed.

Figure 2(a) presents the temperature dependencies of the electrical resistivity measured in different magnetic fields oriented along the c axis with the electric current j flowing within the tetragonal plane, while Fig. 2(b) shows the temperature derivatives of $\rho(T)$. At T_N, the transition temperature to the ordered IC state, the $\rho(T)$ curve changes its slope and shows a distinct bend. T_N is identified as a kink in the $\rho(T)$ dependence, which corresponds to an inflection in the $d\rho/dT(T)$ or a minimum in the second-order temperature derivative of the electrical resistivity. With magnetic field increasing up to 14 T, T_N only slightly changes its position, in agreement with the magnetization data. In turn, the resistivity drops, associated with the transitions to the AFM state at T_1 (in fields $\mu_0 H < 2$ T) and at T_3 (in $\mu_0 H \geqslant 2$ T), seen as sharp

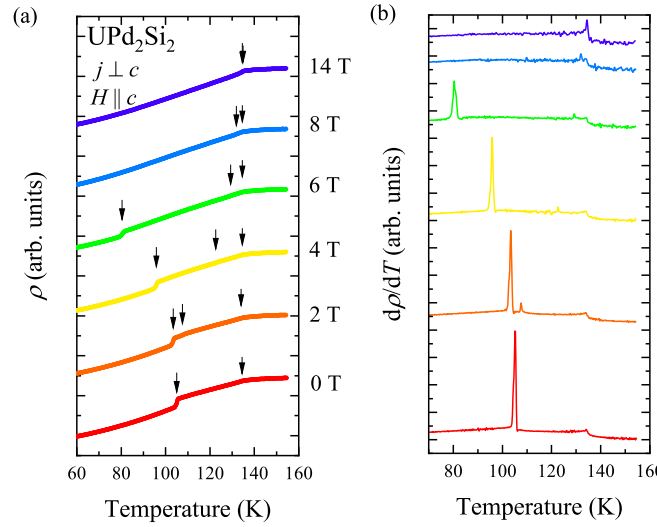

FIG. 2. (a) Temperature dependencies of the electrical resistivity of single-crystalline UPd_2Si_2 measured with electric current flowing perpendicular to the c axis and magnetic field with various magnitudes applied parallel to it. The arrows mark the transition temperatures described in the text. (b) Temperature derivatives of the resistivity data. For clarity, in both panels, the experimental data obtained in different magnetic fields were shifted relative to each other.

pronounced maxima in $d\rho/dT(T)$, shift towards lower temperatures with increasing the magnetic field. In fields stronger than 6 T, the transition at T_3 is no longer observed. At 2 T, another feature appears at a temperature T_2 that is associated with the transition between the IC and FIM phases. It is seen in the $d\rho/dT(T)$ curves as a small maximum that shifts with increasing field towards higher temperatures, with a tendency to merge with the anomaly marking T_N.

The field dependencies of the magnetization, $M(H)$, in single-crystalline UPd_2Si_2 measured at various constant temperatures below and above T_1 are shown in Figs. 3(a)–3(c), respectively. For both temperature regions, distinct metamagneticlike transitions can be seen. At low temperatures, a sharp increase in $M(H)$ marks the transition from the AFM state to the FIM state, which bears a first-order character. At 10 K, the associated hysteresis loop in $M(H)$ is very wide and nearly rectangular. As seen in Fig. 3(a), with increasing temperature, the loop width initially decreases. With a further increase of the temperature the anomaly shifts towards lower fields [see Fig. 3(b)]. In turn, above T_1 [see Fig. 3(c)], the metamagnetic transition from the IC phase to the FIM state is characterized by fairly narrow hysteresis in $M(H)$, and its position moves towards higher fields with increasing temperature.

Figures 4(a) and 4(b) present the field dependencies of the transverse magnetoresistivity, MR(H), of single-crystalline UPd_2Si_2, defined as $\mathrm{MR}(H) = \frac{\rho(H)-\rho(H=0)}{\rho(H=0)}$, measured at constant temperatures, below and above T_1, respectively, with electric current flowing within the tetragonal plane and in magnetic field oriented along the c axis. At low temperatures, the transition between the AFM and FIM states manifests itself as a rapid increase in MR. At 20 K, the hysteresis loop is wide and nearly rectangular. As in the field dependencies

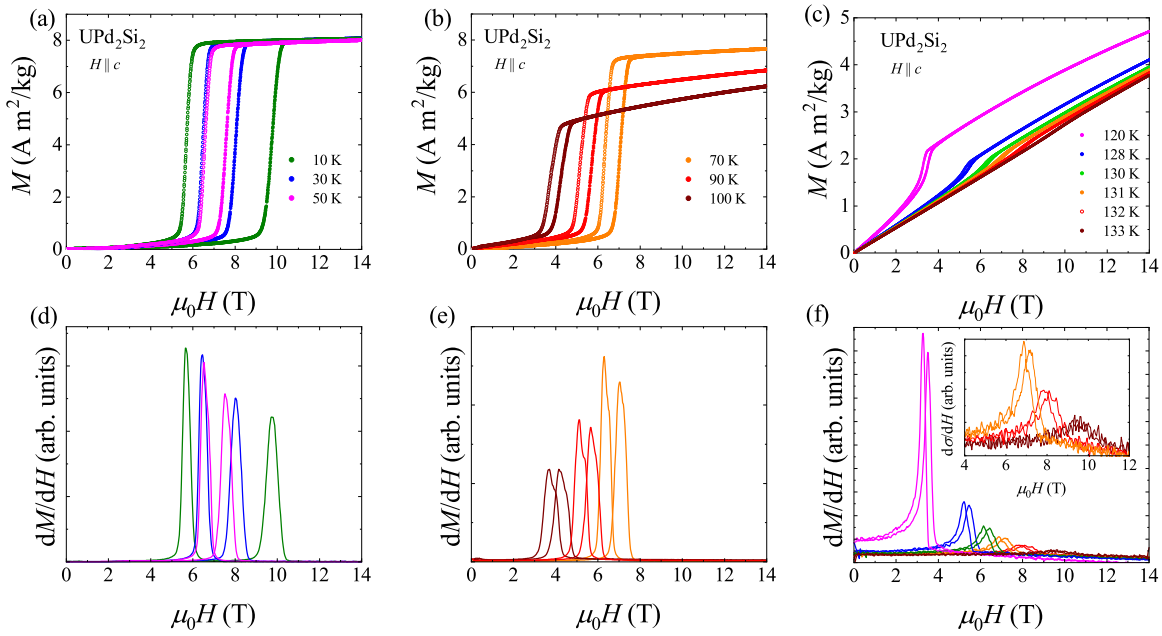

FIG. 3. (a)–(c) The magnetization in single-crystalline UPd_2Si_2 measured as a function of the external magnetic field applied parallel to the c axis at several temperatures (a), (b) below and (c) above T_1 with increasing (solid symbols) and decreasing (open symbols) magnetic field. (d)–(f) Field derivatives of the magnetization data. The inset in (f) presents the zoomed-in dM/dT variations taken above T_1.

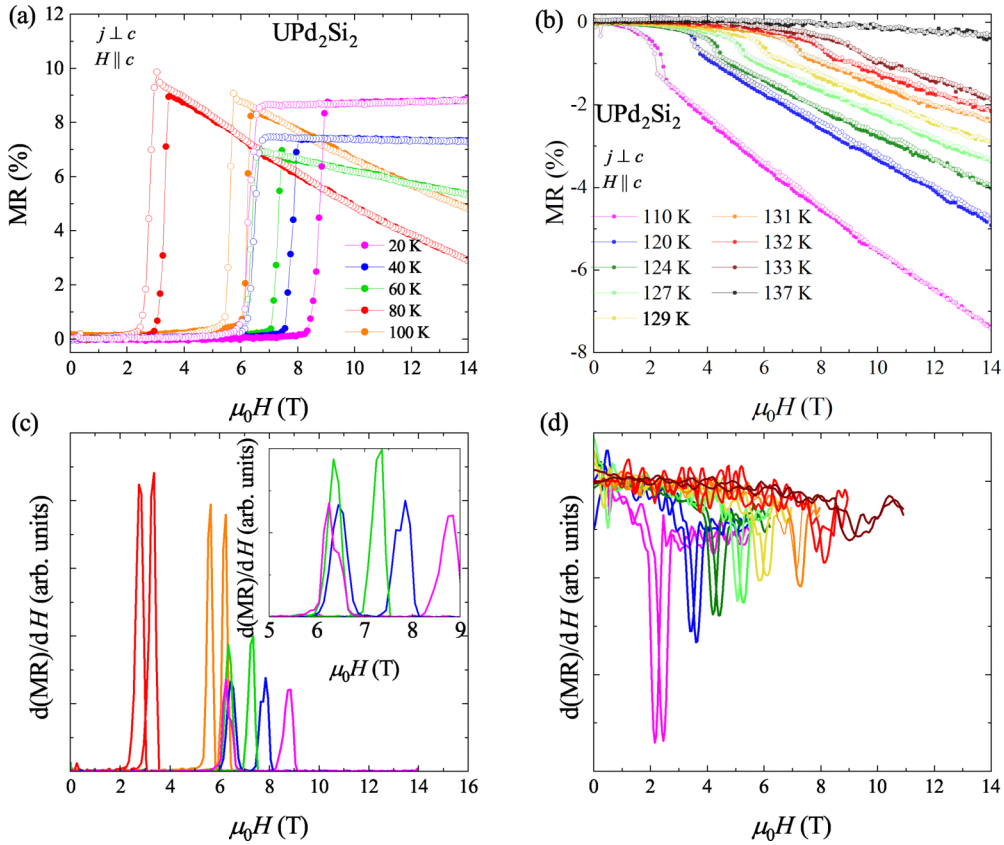

FIG. 4. (a) and (b) Field dependencies of the transverse magnetoresistivity of single-crystalline UPd_2Si_2 measured at several temperatures (a) below and (b) above T_1 with increasing (solid symbols) and decreasing (open symbols) magnetic field applied parallel to the c axis with electric current flowing in the tetragonal plane. (c) and (d) Field derivatives of the magnetoresistivity data taken below and above T_1, respectively. The inset to (c) shows zoomed-in derivatives at 20, 40, and 60 K.

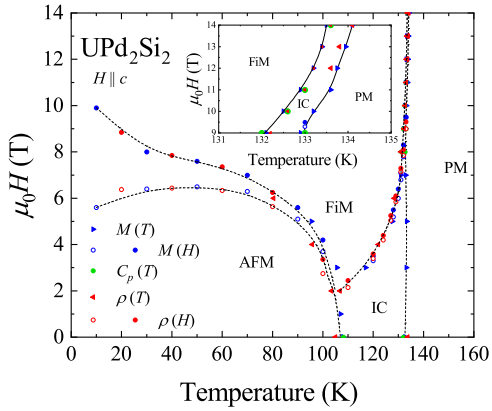

FIG. 5. Magnetic phase diagram of single-crystalline UPd_2Si_2 for an external magnetic field directed along the crystallographic c axis. For the boundary lines determined from the field dependencies of the magnetization and resistivity, the data taken with increasing and decreasing magnetic field strength were used, marked by solid and open symbols, respectively. The inset is the magnification of the high magnetic field region.

of the magnetization, the loops in MR(H) gradually become narrower and shift towards lower fields, when temperature increases. Above T_1, the transition between the IC and FIM phases manifests itself as a drop in MR(H). In the high-temperature region, the hysteresis loops are narrower and the critical field shifts towards higher values with increasing temperature. Finally, the magnetoresistivity isotherm taken at 137 K does not show any singularity, confirming that the compound is in the paramagnetic state.

IV. MAGNETIC PHASE DIAGRAM

Based on the thermodynamic and electrical transport data collected on single-crystalline UPd_2Si_2 in magnetic fields oriented along the crystallographic c axis, the magnetic phase diagram was constructed (see Fig. 5). In weak fields, the compound undergoes two magnetic phase transitions: at T_N from the PM state to the IC state, and at T_1 to the AFM state. The values of T_N were determined as kinks in $M(T)$ and $\rho(T)$. In turn, T_1 was defined as an inflection point on the lower-temperature slope of $M(T)$ and an inflection point in $\rho(T)$ [i.e., pronounced peak in $d\rho(T)/dT$].

Near T_1 and in magnetic fields stronger than 1 T, the occurrence of the FIM phase was established. With decreasing temperature, the transition from the AFM state to the FIM state takes place in a critical field of systematically larger strength. At the same time, a hysteresis width associated with this transition rapidly grows. For each temperature T_3, the critical fields were derived by inspecting the first field derivatives

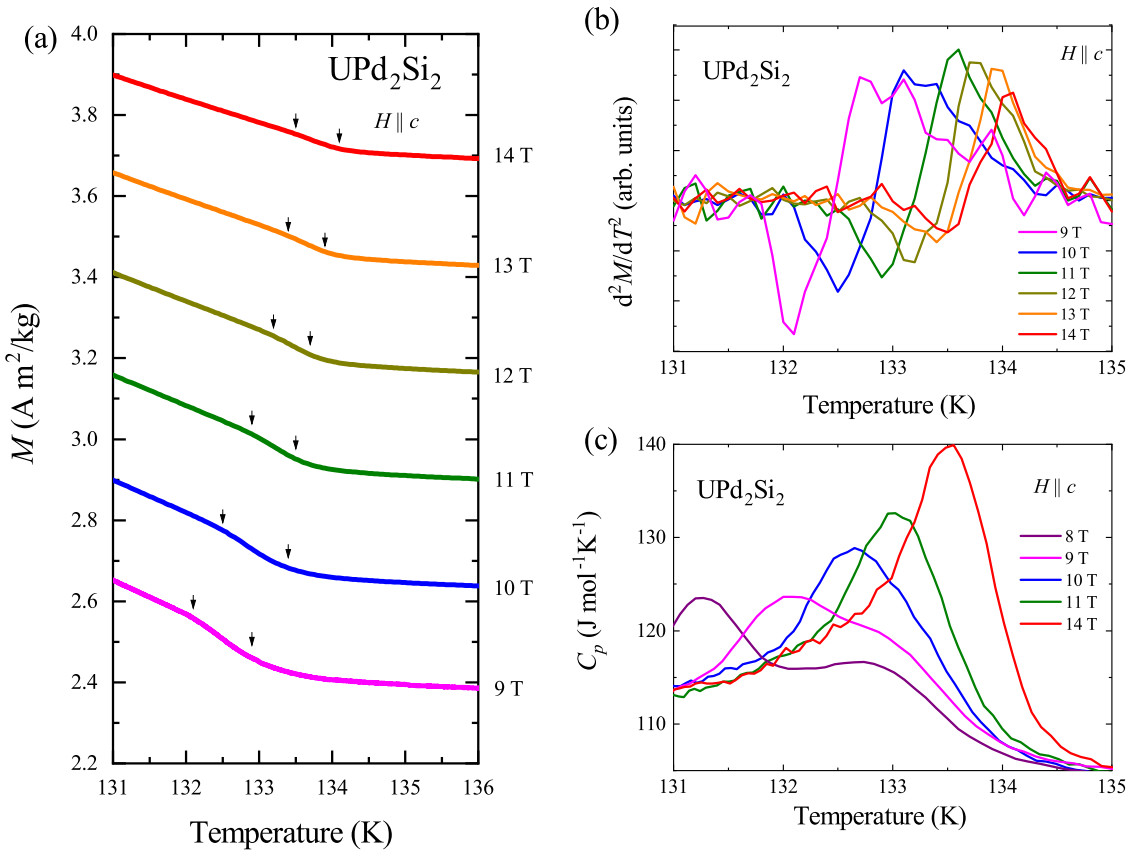

FIG. 6. (a) Temperature dependencies of the magnetization in single-crystalline UPd_2Si_2 measured in strong magnetic fields applied along the c axis at temperatures close to T_N. The arrows mark the magnetic transition temperatures. (b) Second-order temperature derivatives of the magnetization data. (c) Temperature variations of the specific heat of single-crystalline UPd_2Si_2 measured in strong magnetic fields applied along the c axis at temperatures close to T_N.

of $M(H)$ [see Figs. 3(d) and 3(e)] and MR(H) [see Fig. 4(c)]. The phase boundary setting the changes in T_3 was established also by analyzing the position of a inflection point on the lower-temperature slope of $M(T)$ and a peak in $d\rho/dT$.

At temperatures higher than T_1, UPd_2Si_2 undergoes the transition from the IC state to the FIM state. The phase boundary labeled as T_2 was defined as higher-temperature kinks in $M(T)$ [minima in second-order derivatives $d^2M(T)/dT^2$] and small maxima in the temperature derivatives of the electrical resistivity. The critical field of the IC-FIM transition was determined also by analyzing the first field derivatives of $M(H)$ and MR(H) above T_1 [see Figs. 3(f) and 4(d)].

As can be inferred from Fig. 5, at about 106 K near a field of about 2 T, there occurs in the magnetic phase diagram of UPd_2Si_2 a triple point at which three ordered phases IC, FIM, and AFM meet. This finding corroborates the prior observation by Honma *et al.* [24].

Another mulitcritical point in the H-T diagram of UPd_2Si_2, possibly of the LP character (viz., the Introduction) may be expected in strong magnetic fields, where T_2 would merge with T_N. To address this most tempting issue, the magnetization, specific heat, and electrical resistivity data taken for UPd_2Si_2 in high magnetic fields were thoroughly inspected. Figure 6(a) shows the temperature dependencies of the magnetization at temperatures and magnetic fields close to the hypothetical LP. The magnetization was measured with increasing temperature, and T_2 was defined as a kink in $M(T)$, well seen as a minimum in the second-order temperature derivative $d^2M(T)/dT^2$ [see Fig. 6(b)]. Clearly, T_2 shifts towards higher temperatures with increasing the magnetic field strength. However, as displayed in the inset to Fig. 5, simultaneously also T_N [determined as a maximum in $d^2M(T)/dT^2$] increases slightly and in consequence the boundary lines between the FIM-IC phases and the IC-PM phases do not meet up to 14 T, the strongest field available in our experiments.

The specific heat measured with increasing temperature in high magnetic fields is shown in Fig. 6(c). At 8 and 9 T, the two phase transitions are clearly separated, but in stronger magnetic fields they are very close to each other. As the position of the maxima in fields $\mu_0 H > 9$ T coincides with T_2 determined from the magnetization data, one can assume that the anomaly related to T_N is hidden in the high-temperature slope of the maximum. Indeed, the maxima are asymmetric and a small hump in the high-temperature slope of these maxima can be recognized.

The temperature variations of the electrical resistivity measured in strong magnetic fields and their temperature derivatives are presented in Figs. 7(a) and 7(b), respectively. The critical temperature T_2, defined as an inflection point in $\rho(T)$ and a maximum in $d\rho/dT(T)$, increases monotonically with increasing magnetic field. At the same time, T_N, represented as a bend in the $\rho(T)$ variation, also increases. As a result, the two transition lines do not meet up to 14 T, confirming the finding from the high-field magnetization and specific-heat data.

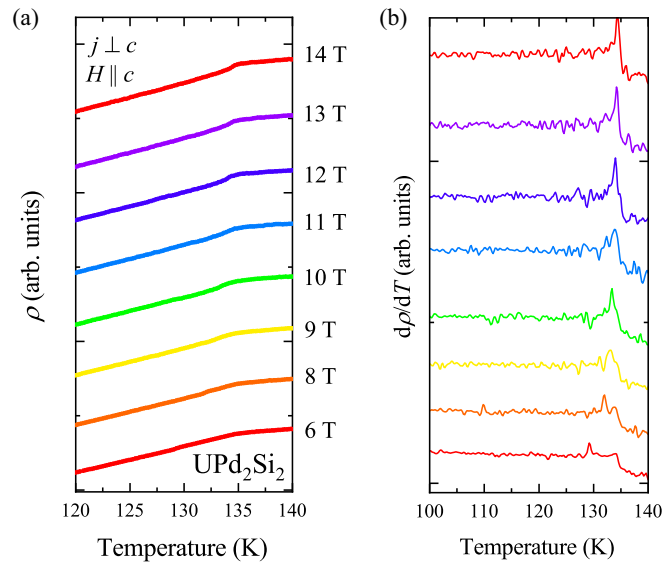

FIG. 7. (a) Temperature dependencies of the electrical resistivity of single-crystalline UPd_2Si_2 measured in strong magnetic fields at temperatures close to T_N with electric current flowing perpendicular to the c axis and magnetic field applied parallel to it. (b) Temperature derivatives of the resistivity data. For clarity, in both figures, the curves measured in different fields were shifted relative to each other.

V. CONCLUSIONS

A single crystal of UPd_2Si_2 was studied in wide ranges of magnetic field and temperatures. Using the collected data, the magnetic H-T phase diagram for a magnetic field applied along the c axis was constructed. Below the Néel temperature of 132 K, the compound undergoes a magnetic phase transition to the incommensurately modulated state. A further decrease of the temperature results in the formation of the uniform antiferromagnetic structure below 108 K. In strong magnetic fields, one observes stabilization of the ferrimagnetic phase. A triple point, in which the three ordered phases meet, is observed at about 106 K near 2 T. With increasing the magnetic field strength, the domain of the incommensurately modulated phase gets narrower, which may result in the occurrence of a Lifshitz point at the merging of the paramagnetic phase with two different ordered phases, one of them being incommensurate and the other of ferrimagnetic character. However, in the experimental study performed in this work no such multicritical point was found up to 14 T. Hypothetically, stronger magnetic fields are required to observe LP in UPd_2Si_2 at ambient pressure. A different scenario may possibly be realized in pressurized samples, and this issue will be addressed in our companion paper [29].

ACKNOWLEDGMENTS

The work was supported by Narodowe Centrum Nauki (National Science Center, Poland) within scientific project SONATA-14 2018/31/D/ST3/03295.

[1] R. M. Hornreich, M. Luban, and S. Shtrikman, Critical behavior at the onset of $\vec{k}$-space instability on the λ line, Phys. Rev. Lett. **35**, 1678 (1975).

[2] R. Hornreich, The Lifshitz point: Phase diagrams and critical behavior, J. Magn. Magn. Mater. **15-18**, 387 (1980).

[3] Y. Shapira, C. C. Becerra, N. F. Oliveira, and T. S. Chang, Phase diagram, susceptibility, and magnetostriction of MnP: Evidence for a Lifshitz point, Phys. Rev. B **24**, 2780 (1981).

[4] A. Szytuła, Magnetic properties of 1:2:2 rare-earth and actinide intermetallics, J. Alloys Compd. **181**, 123 (1992).

[5] T. T. M. Palstra, A. A. Menovsky, G. J. Nieuwenhuys, and J. A. Mydosh, Magnetic properties of the ternary compounds CeT_2Si_2 and UT_2Si_2, J. Magn. Magn. Mater. **54**, 435 (1986).

[6] Y. Dalichaouch, M. B. Maple, M. S. Torikachvili, and A. L. Giorgi, Ferromagnetic instability in the heavy-electron compound URu_2Si_2 doped with Re or Tc, Phys. Rev. B **39**, 2423 (1989).

[7] J. A. Mydosh, P. M. Oppeneer, and P. S. Riseborough, Hidden order and beyond: an experimental—theoretical overview of the multifaceted behavior of URu_2Si_2, J. Phys.: Condens. Matter **32**, 143002 (2020).

[8] T. D. Matsuda, N. Metoki, Y. Haga, S. Ikeda, K. Kaneko, E. Yamamoto, and Y. Ōnuki, Crystal and magnetic structure in the itinerant $5f$ antiferromagnet UCr_2Si_2, J. Phys.: Condens. Matter **15**, S2023 (2003).

[9] T. D. Matsuda, N. Metoki, Y. Haga, S. Ikeda, T. Okubo, K. Sugiyama, N. Nakamura, K. Kindo, K. Kaneko, A. Nakamura, E. Yamamoto, and Y. Ōnuki, Single crystal growth and structural and magnetic properties of the uranium ternary intermetallic compound UCr_2Si_2, J. Phys. Soc. Jpn. **72**, 122 (2003).

[10] A. Szytuła, S. Siek, J. Leciejewicz, A. Zygmunt, and Z. Ban, Neutron diffraction study of UT_2X_2 (T = Mn, Fe, X = Si, Ge) intermetallic systems, J. Phys. Chem. Solids **49**, 1113 (1988).

[11] L. Chełmicki, J. Leciejewicz, and A. Zygmunt, Magnetic properties of UT_2Si_2 and UT_2Ge_2 (T = Co, Ni, Cu) intermetallic systems, J. Phys. Chem. Solids **46**, 529 (1985).

[12] P. Svoboda, P. Javorský, V. Sechovský, A. Menovsky, M. Hofmann, and N. Stüsser, Magnetic phase diagram and critical scattering of UNi_2Si_2, Phys. B: Condens. Matter **322**, 248 (2002).

[13] T. D. Matsuda, Y. Haga, S. Ikeda, A. Galatanu, E. Yamamoto, H. Shishido, M. Yamada, J.-I. Yamaura, M. Hedo, Y. Uwatoko, T. Matsumoto, T. Tada, S. Noguchi, T. Sugimoto, K. Kuwahara, K. Iwasa, M. Kohgi, R. Settai, and Y. Ōnuki, Electrical and magnetic properties of a single crystal UCu_2Si_2, J. Phys. Soc. Jpn. **74**, 1552 (2005).

[14] R. Troć, Z. Gajek, A. Pikul, H. Misiorek, E. Colineau, and F. Wastin, Phenomenological crystal-field model of the magnetic and thermal properties of the Kondo-like system UCu_2Si_2, Phys. Rev. B **88**, 024416 (2013).

[15] A. J. Dirkmaat, T. Endstra, E. A. Knetsch, G. J. Nieuwenhuys, J. A. Mydosh, A. A. Menovsky, F. R. de Boer, and Z. Tarnawski, Magnetic, thermal, and transport properties of UIr_2Si_2, Phys. Rev. B **41**, 2589 (1990).

[16] R. A. Steeman, E. Frikkee, S. A. M. Mentink, A. A. Menovsky, G. J. Nieuwenhuys, and J. A. Mydosh, Hybridisation effects in UPt_2Si_2, J. Phys.: Condens. Matter **2**, 4059 (1990).

[17] C. Tabata, N. Miura, K. Uhlířova, M. Vališka, H. Saito, H. Hidaka, T. Yanagisawa, V. Sechovský, and H. Amitsuka, Peculiar magnetism of UAu_2Si_2, Phys. Rev. B **94**, 214414 (2016).

[18] A. Vernière, S. Raymond, J. Boucherle, P. Lejay, B. Fåk, J. Flouquet, and J. Mignot, Magnetic structure and physical properties of the heavy fermion UIr_2Si_2, J. Magn. Magn. Mater. **153**, 55 (1996).

[19] A. Vernière, P. Lejay, J. Boucherle, J. Muller, S. Raymond, J. Flouquet, and A. Sulpice, Low temperature structural and physical behaviour of UIr_2Si_2 single crystal, Phys. B: Condens. Matter **206**, 509 (1995).

[20] M. Szlawska, M. Majewicz, D. A. Kowalska, and D. Kaczorowski, Metamagnetic transition in single-crystalline UIr_2Si_2, Sci. Rep. **13**, 14772 (2023).

[21] A. Amorese, M. Sundermann, B. Leedahl, A. Marino, D. Takegami, H. Gretarsson, A. Gloskovskii, C. Schlueter, M. W. Haverkort, Y. Huang, M. Szlawska, D. Kaczorowski, S. Ran, M. B. Maple, E. D. Bauer, A. Leithe-Jasper, P. Hansmann, P. Thalmeier, L. H. Tjeng, and A. Severing, From antiferromagnetic and hidden order to Pauli paramagnetism in UM_2Si_2 compounds with $5f$ electron duality, Proc. Natl. Acad. Sci. USA **117**, 30220 (2020).

[22] B. Shemirani, H. Lin, M. F. Collins, C. V. Stager, J. D. Garrett, and W. J. L. Buyers, Magnetic structure of UPd_2Si_2, Phys. Rev. B **47**, 8672 (1993).

[23] M. F. Collins, B. Shemirani, C. V. Stager, J. D. Garrett, H. Lin, W. J. L. Buyers, and Z. Tun, Magnetic structure of UPd_2Si_2 in a magnetic field, Phys. Rev. B **48**, 16500 (1993).

[24] T. Honma, H. Amitsuka, S. Yasunami, K. Tenya, T. Sakakibara, H. Mitamura, T. Goto, G. Kido, S. Kawarazaki, Y. Miyako, K. Sugiyama, and M. Date, Incommensurate-commensurate magnetic phase transitions of the Ising-$5f$ system UPd_2Si_2: The H-T phase diagram and mean-field analyses, J. Phys. Soc. Jpn. **67**, 1017 (1998).

[25] H. Ptasiewicz-Bąk, J. Leciejewicz, and A. Zygmunt, Neutron diffraction study of magnetic ordering in UPd_2Si_2, UPd_2Ge_2, URh_2Si_2 and URh_2Ge_2, J. Phys. F: Met. Phys. **11**, 1225 (1981).

[26] T. Plackowski, D. Kaczorowski, and J. Sznajd, Magnetic phase diagram and possible Lifshitz critical point in UPd_2Si_2, Phys. Rev. B **83**, 174443 (2011).

[27] G. Quirion, F. S. Razavi, M. L. Plumer, and J. D. Garrett, Pressure-temperature phase diagram of UPd_2Si_2 and UNi_2Si_2, Phys. Rev. B **57**, 5220 (1998).

[28] H. Hidaka, A. Tanaka, S. Takahashi, T. Yanagisawa, and H. Amitsuka, Pressure-induced bicritical point in UPd_2Si_2, J. Phys.: Conf. Ser. **273**, 012032 (2011).

[29] M. Szlawska, M. Majewicz, M. Ohashi, and D. Kaczorowski, following paper, Hunt for a Lifshitz point in single-crystalline UPd_2Si_2. II. High pressures, Phys. Rev. B **110**, 014435 (2024).